

Electronic Supplementary Information (ESI) for

Unsymmetrical Nonplanar ‘Push-Pull’ β -Octasubstituted Porphyrins: Facile Synthesis, Structural, Photophysical and Electrochemical Redox Properties

Pinki Rathi,^a Ray Butcher^b and Muniappan Sankar*^a

^aDepartment of Chemistry, Indian Institute of Technology Roorkee, Roorkee-247667, India

^bDepartment of Chemistry, Howard University, Washington, DC 20059, USA

Table of Contents

	Page No.
Figure S1. ^1H NMR spectrum $\text{H}_2\text{TPP}(\text{Ph})_2\text{Br}_6$ in CDCl_3 at 298K.	3
Figure S2. ^1H NMR spectrum $\text{NiTPP}(\text{Ph})_2\text{Br}_6$ in CDCl_3 at 298K.	3
Figure S3. ^1H NMR spectrum $\text{ZnTPP}(\text{Ph})_2\text{Br}_6$ in CDCl_3 at 298K.	4
Figure S4. ^1H NMR spectrum $\text{H}_2\text{TPP}(\text{NO}_2)(\text{Ph})_2\text{Br}_5$ in CDCl_3 at 298K.	4
Figure S5. ^1H NMR spectrum $\text{NiTPP}(\text{NO}_2)(\text{Ph})_2\text{Br}_5$ in CDCl_3 at 298K.	5
Figure S6. ^1H NMR spectrum $\text{ZnTPP}(\text{NO}_2)(\text{Ph})_2\text{Br}_5$ in CDCl_3 at 298K.	5
Figure S7. ^{13}C NMR spectrum of $\text{H}_2\text{TPP}(\text{Ph})_2\text{Br}_6$ in CDCl_3 at 298 K.	6
Figure S8. ^{13}C NMR spectrum of $\text{H}_2\text{TPP}(\text{NO}_2)(\text{Ph})_2\text{Br}_6$ in CDCl_3 at 298 K.	6
Figure S9. MALDI-TOF mass spectrum of $\text{H}_2\text{TPP}(\text{Ph})_2\text{Br}_6$.	7
Figure S10. MALDI-TOF mass spectrum of $\text{CoTPP}(\text{Ph})_2\text{Br}_6$.	7
Figure S11. MALDI-TOF mass spectrum of $\text{NiTPP}(\text{Ph})_2\text{Br}_6$.	8
Figure S12. MALDI-TOF mass spectrum of $\text{CuTPP}(\text{Ph})_2\text{Br}_6$.	8
Figure S13. MALDI-TOF mass spectrum of $\text{ZnTPP}(\text{Ph})_2\text{Br}_6$.	9
Figure S14. MALDI-TOF mass spectrum of $\text{H}_2\text{TPP}(\text{NO}_2)(\text{Ph})_2\text{Br}_5$.	9
Figure S15. MALDI-TOF mass spectrum of $\text{CoTPP}(\text{NO}_2)(\text{Ph})_2\text{Br}_5$.	10
Figure S16. MALDI-TOF mass spectrum of $\text{NiTPP}(\text{NO}_2)(\text{Ph})_2\text{Br}_5$.	10
Figure S17. MALDI-TOF mass spectrum of $\text{CuTPP}(\text{NO}_2)(\text{Ph})_2\text{Br}_5$.	11
Figure S18. MALDI-TOF mass spectrum of $\text{ZnTPP}(\text{NO}_2)(\text{Ph})_2\text{Br}_5$.	11
Table S1. Crystallographic data of $\text{H}_2\text{TPP}(\text{NO}_2)(\text{Ph})_2\text{Br}_5$.	12
Table S2. Selected average bond lengths (\AA) and bond angles ($^\circ$) for the single crystal of $\text{H}_2\text{TPP}(\text{NO}_2)\text{Ph}_2\text{Br}_5$.	13
Figure S19. B3LYP/LANL2DZ- optimized geometry showing the Top views as well as side views of $\text{H}_2\text{TPP}(\text{NO}_2)(\text{Ph})_2\text{Br}_5$ (1a and 1b) and $\text{H}_2\text{TPPPh}_2\text{Br}_6$ (1d and 1e) respectively. The displacement of porphyrin-core atoms from mean plane are shown in figures 1c and 1f for $\text{H}_2\text{TPP}(\text{NO}_2)(\text{Ph})_2\text{Br}_5$ and $\text{H}_2\text{TPP}(\text{Ph})_2\text{Br}_6$ respectively.	14
Table S3. Selected bond lengths (\AA) and bond angles ($^\circ$) for the B3LYP/LANL2DZ optimized geometries of $\text{H}_2\text{TPP}(\text{Ph})_2\text{Br}_5\text{X}$ ($\text{X} = \text{NO}_2$ or Br).	15

Figure S20. Fluorescence spectra of (a) MTPP(NO_2)(Ph) ₂ Br ₅ and (b) MTPP(Ph) ₂ Br ₆ (M = 2H, Zn (II)) in CH ₂ Cl ₂ at 298 K.	16
Figure S21. UV-visible spectral titration of H ₂ TPP(Ph) ₂ Br ₆ with TFA (a) and TBAOH (b) in toluene at 298 K respectively. insets shows the corresponding Hill plots.	16
Figure S22. Cyclic Voltametric (in V vs Ag/AgCl) traces recorded for porphyrins (a) MTPP(Ph) ₂ Br ₆ (M = 2H, Co(II), Cu(II), Ni(II), Zn(II)) and MTPP(NO_2)(Ph) ₂ Br ₆ (M = 2H, Co(II), Cu(II), Ni(II), Zn(II)) in CH ₂ Cl ₂ containing 0.1 M TBAPF ₆ with a scan rate of 0.1 V/s at 298 K.	17

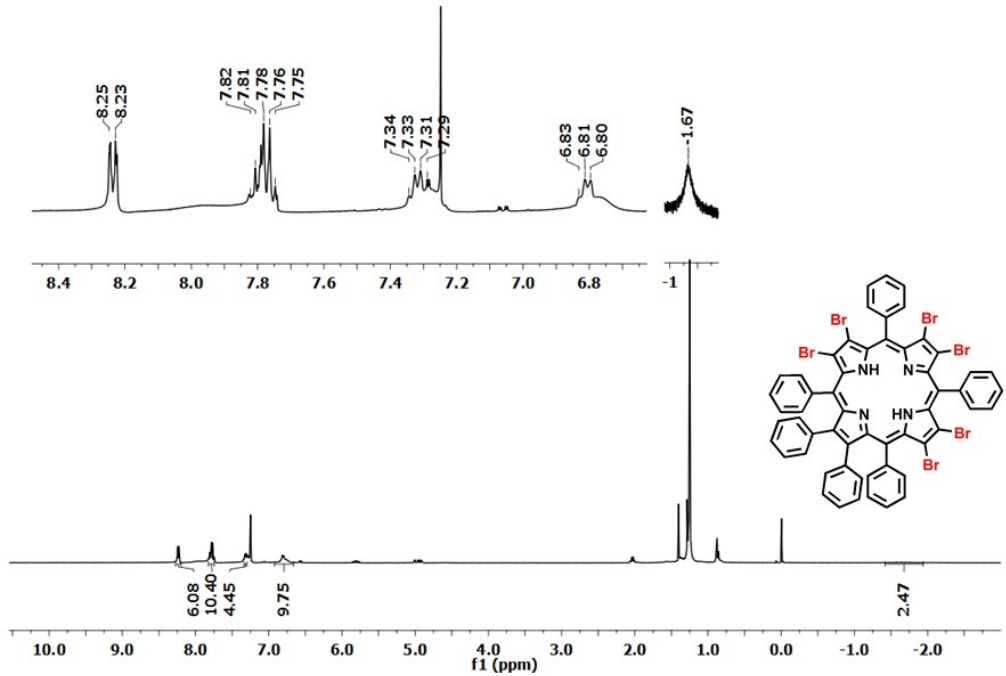


Figure S1. ^1H NMR $\text{H}_2\text{TPP}(\text{Ph})_2\text{Br}_6$ in CDCl_3 at 298K.

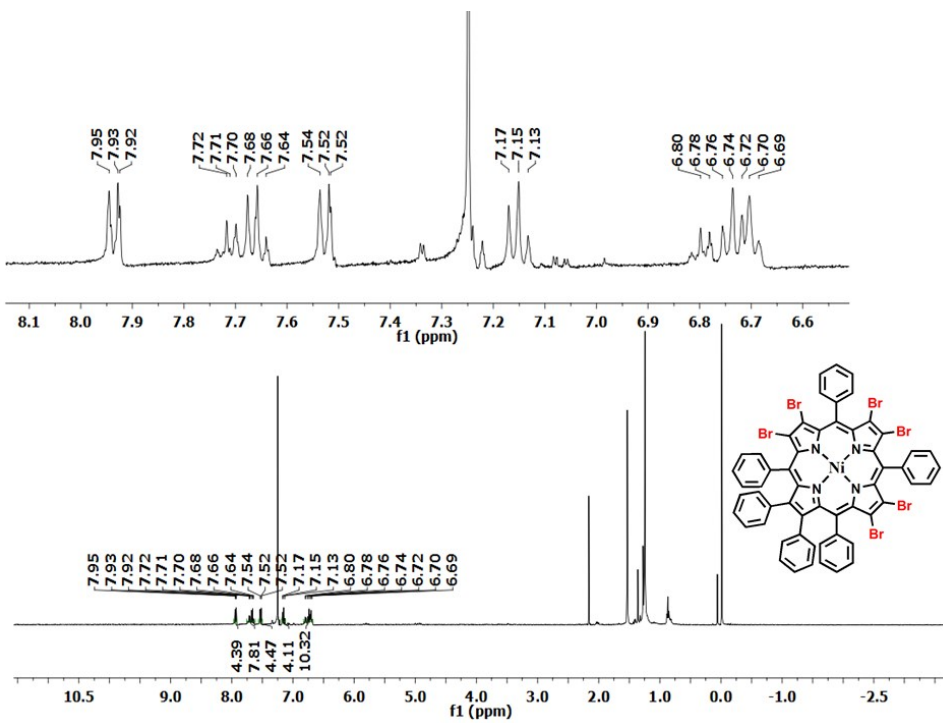


Figure S2. ^1H NMR $\text{NiTPP}(\text{Ph})_2\text{Br}_6$ in CDCl_3 at 298K.

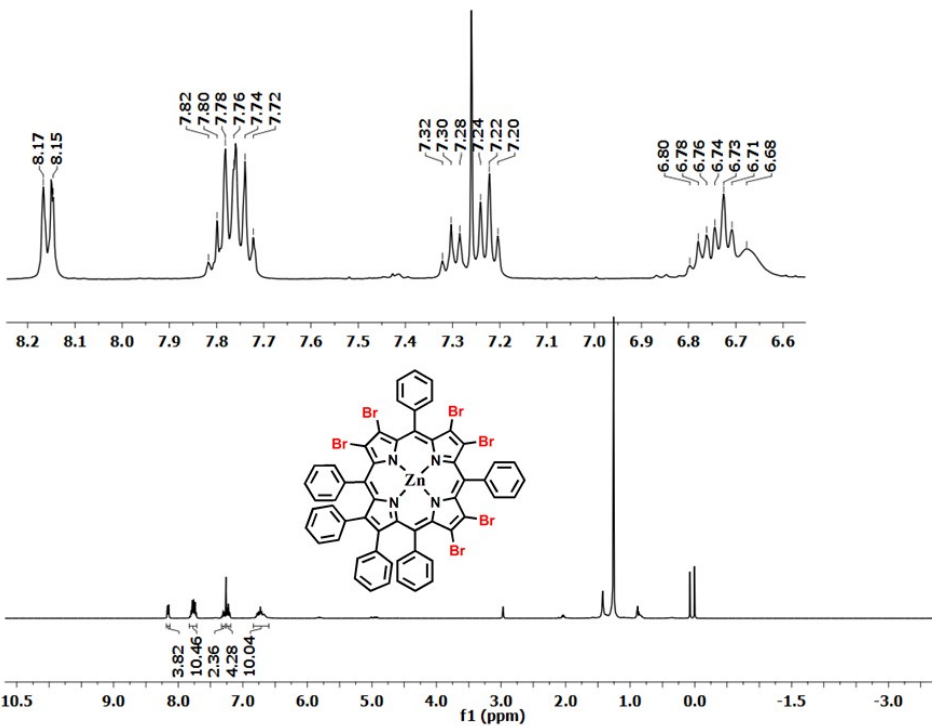


Figure S3. ^1H NMR ZnTPP(Ph)₂Br₆ in CDCl₃ at 298K.

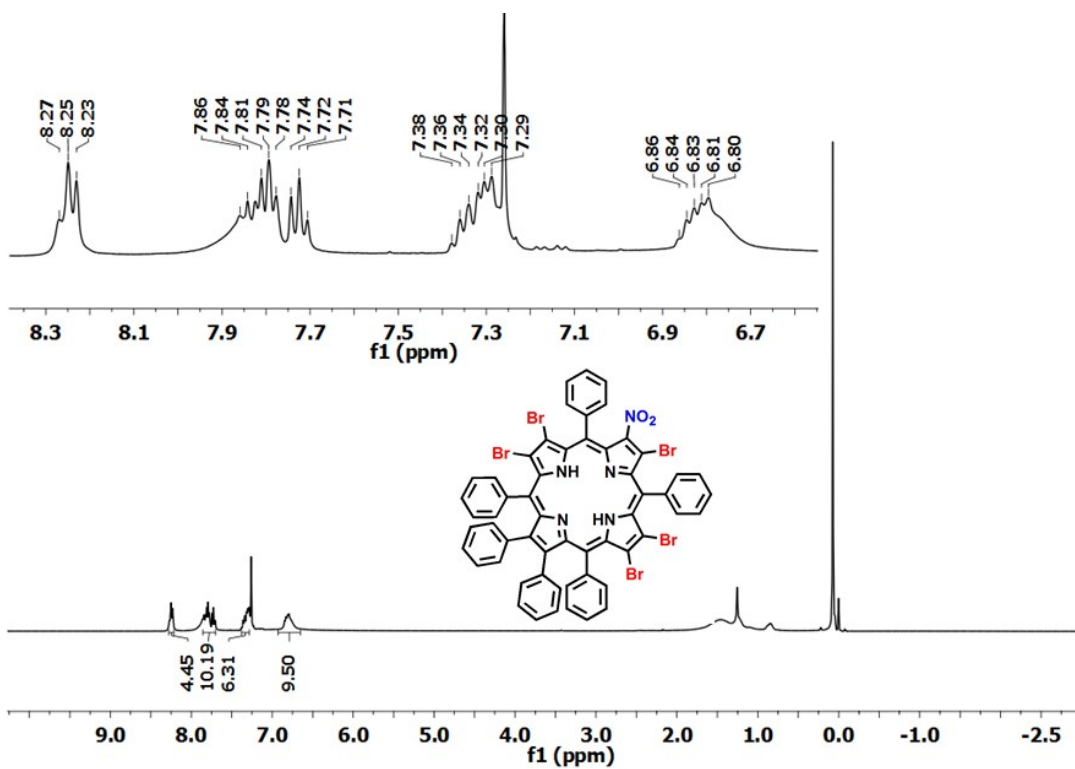


Figure S4. ^1H NMR spectrum of H₂TPP(NO₂)(Ph)₂Br₅ in CDCl₃ at 298 K.

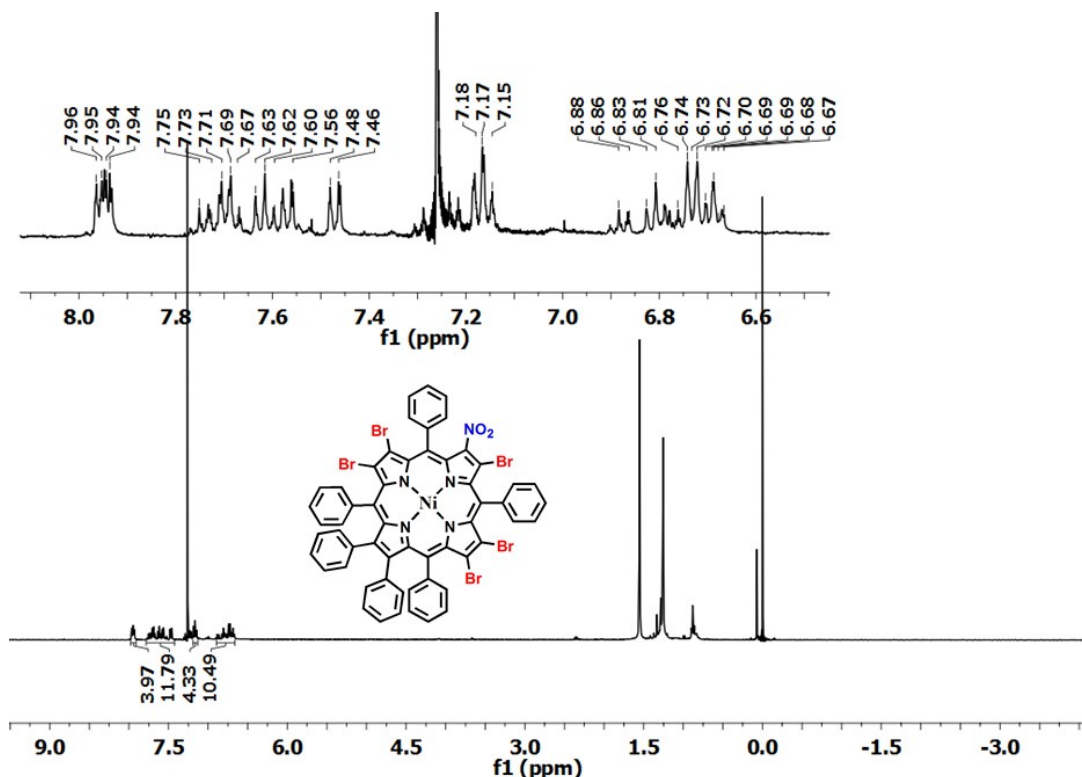


Figure S5. ^1H NMR spectrum of NiTPP(NO_2)(Ph) $_2\text{Br}_5$ in CDCl_3 at 298 K.

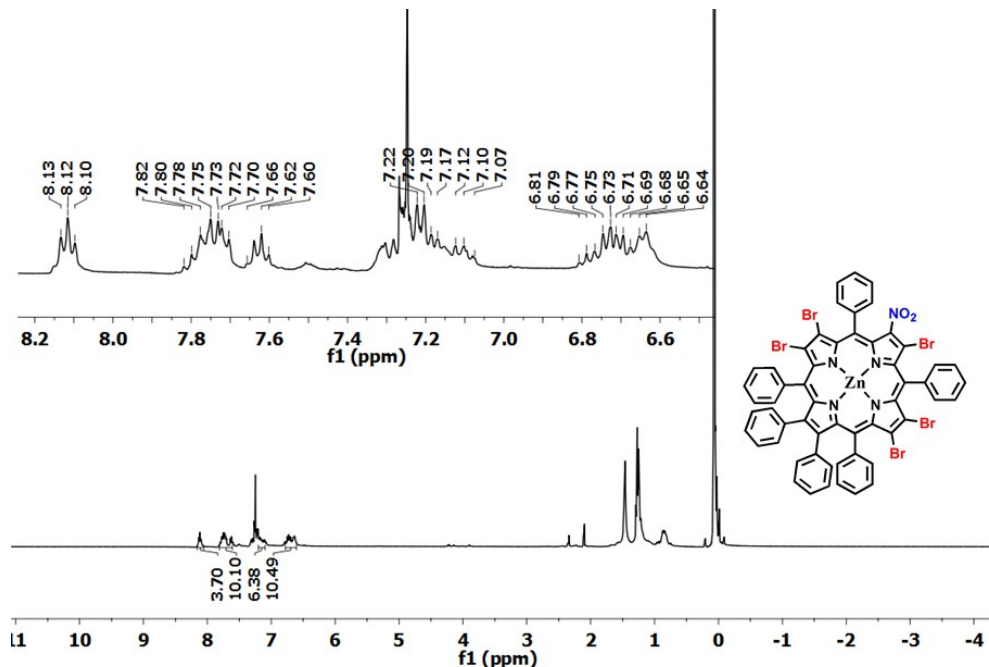


Figure S6. ^1H NMR spectrum of ZnTPP(NO_2)(Ph) $_2\text{Br}_5$ in CDCl_3 at 298 K.

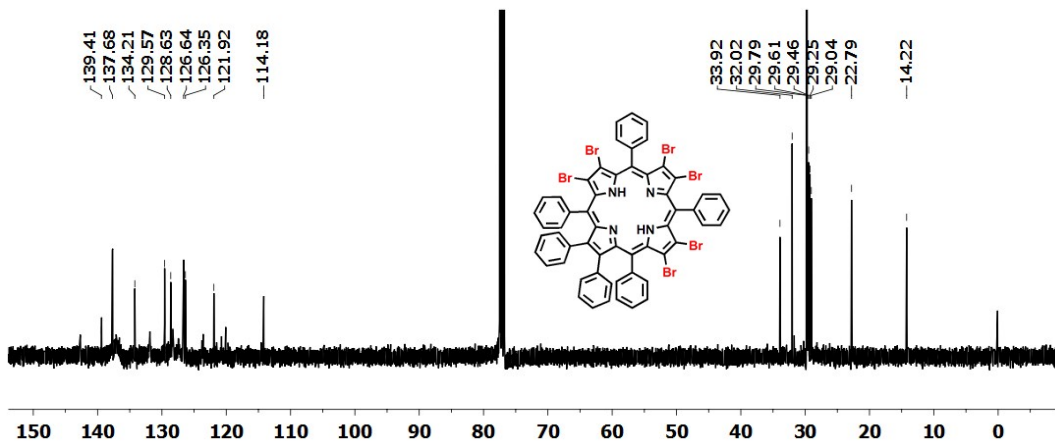


Figure S7. ^{13}C NMR spectrum of $\text{H}_2\text{TPP}(\text{Ph})_2\text{Br}_6$ in CDCl_3 at 298 K.

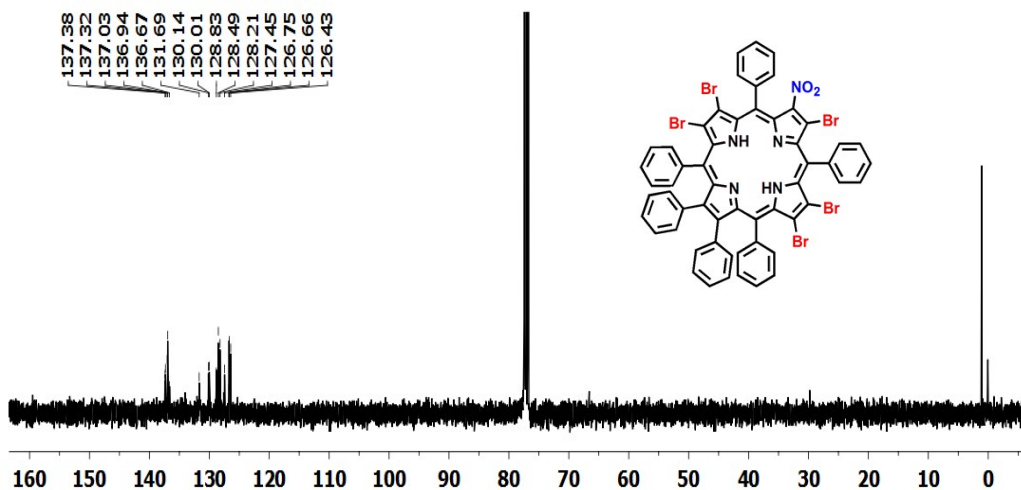


Figure S8. ^{13}C NMR spectrum of $\text{H}_2\text{TPP}(\text{NO}_2)(\text{Ph})_2\text{Br}_5$ in CDCl_3 at 298 K.

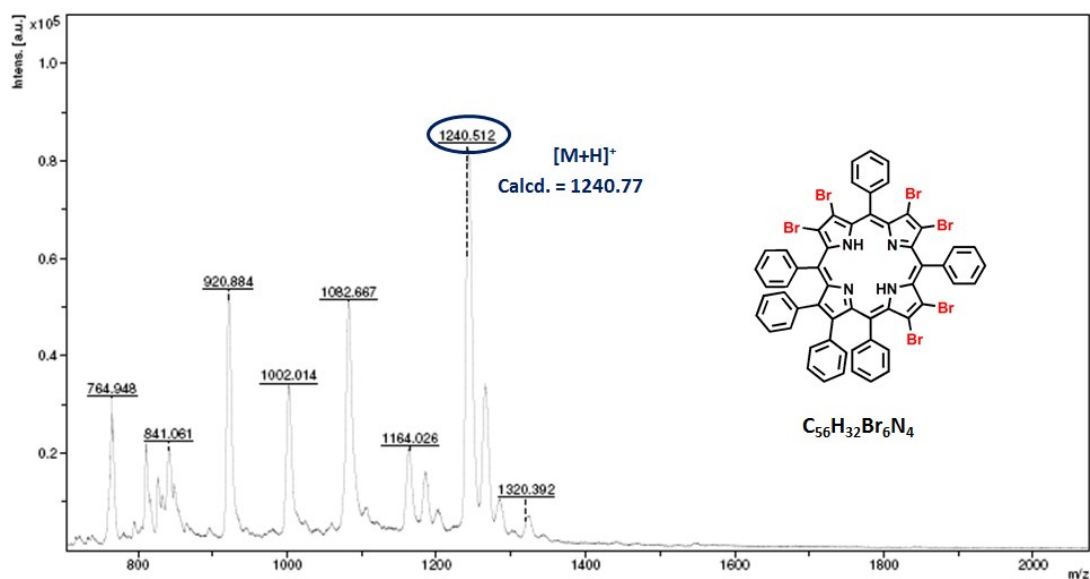


Figure S9. MALDI-TOF mass spectrum of $\text{H}_2\text{TPP}(\text{Ph})_2\text{Br}_6$

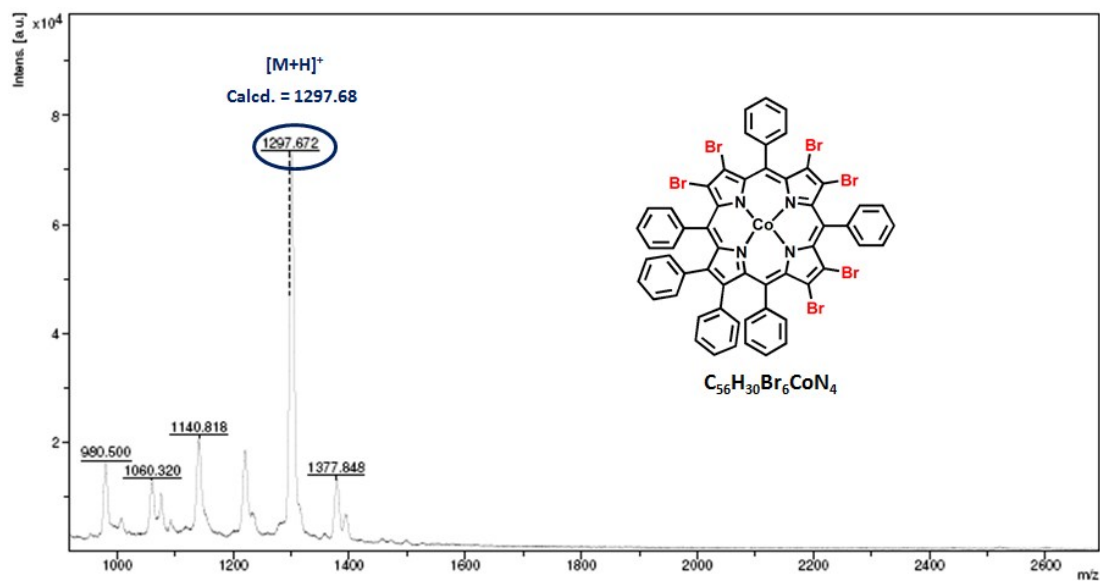


Figure S10. MALDI-TOF mass spectrum of $\text{CoTPP}(\text{Ph})_2\text{Br}_6$.

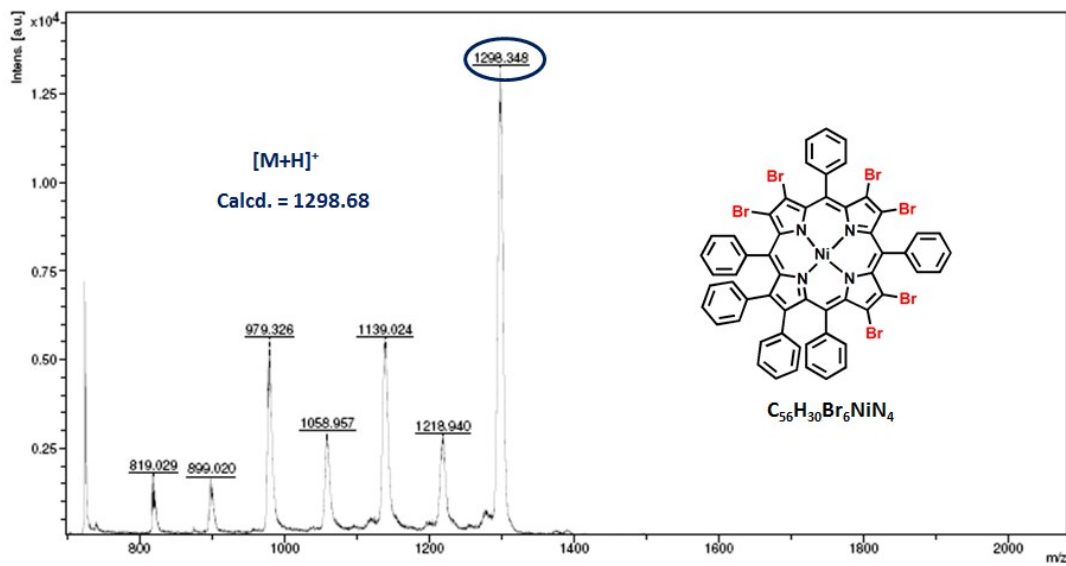


Figure S11. MALDI-TOF mass spectrum of NiTPP(Ph)₂Br₆.

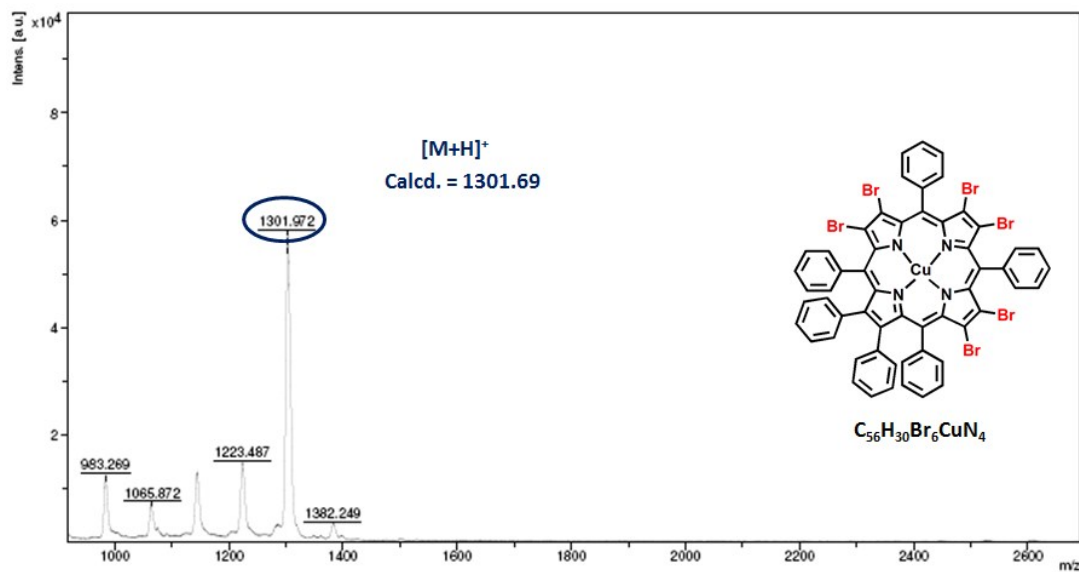


Figure S12. MALDI-TOF mass spectrum of CuTPP(Ph)₂Br₆.

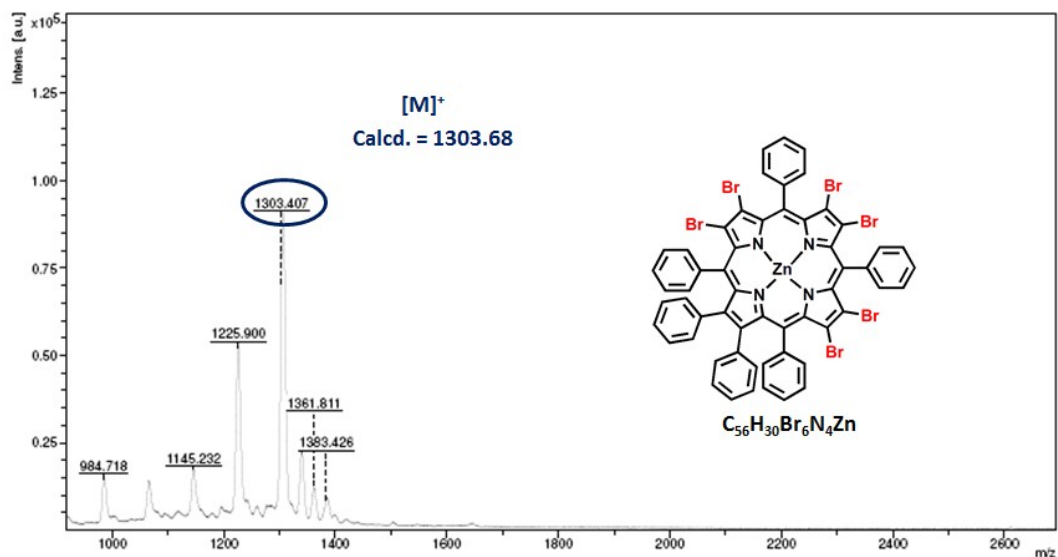


Figure S13. MALDI-TOF mass spectrum of $\text{ZnTPP}(\text{Ph})_2\text{Br}_6$.

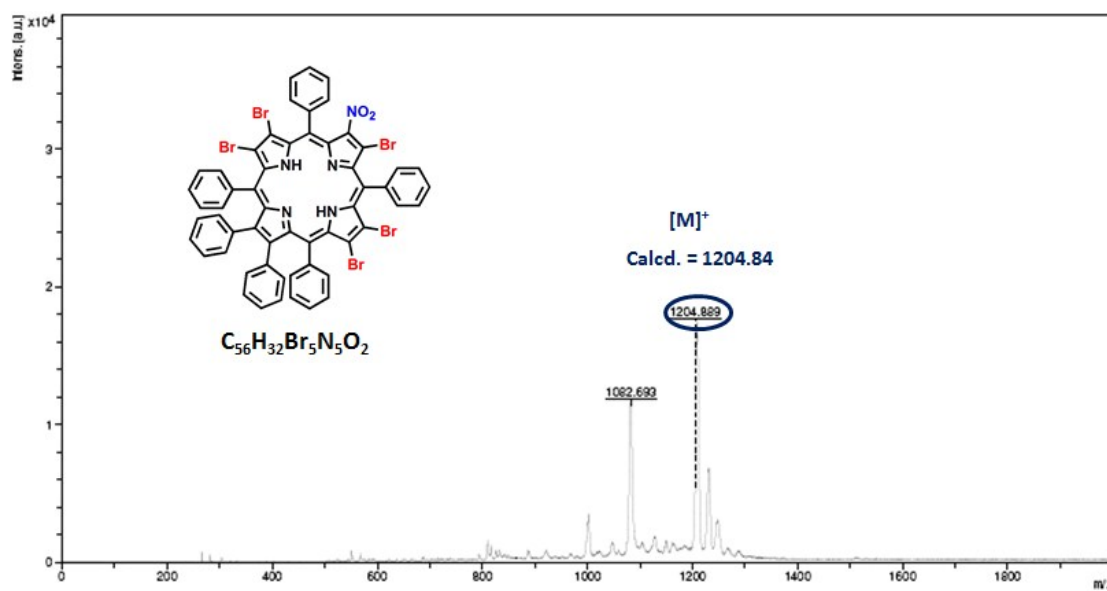


Figure S14. MALDI-TOF mass spectrum of $\text{H}_2\text{TPP}(\text{NO}_2)(\text{Ph})_2\text{Br}_5$.

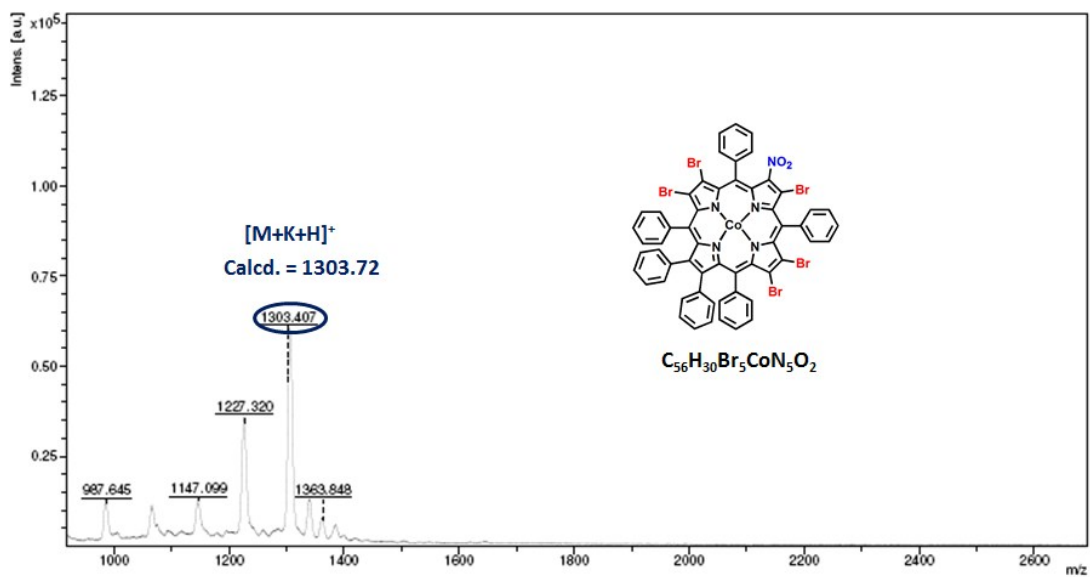


Figure S15. MALDI-TOF mass spectrum of $\text{CoTPP}(\text{NO}_2)(\text{Ph})_2\text{Br}_5$.

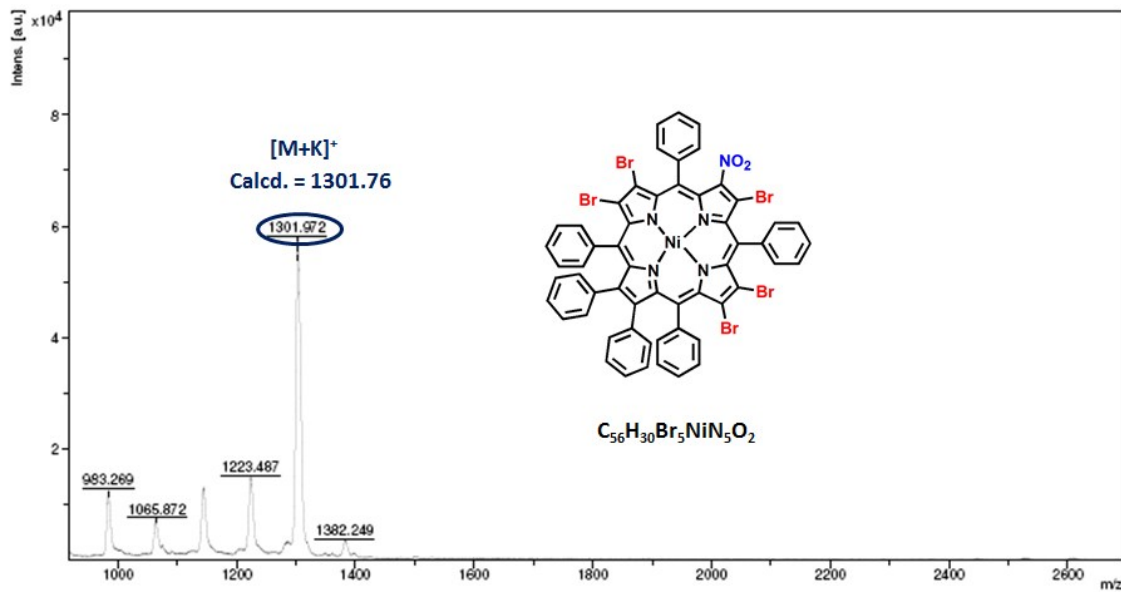


Figure S16. MALDI-TOF mass spectrum of $\text{NiTPP}(\text{NO}_2)(\text{Ph})_2\text{Br}_5$.

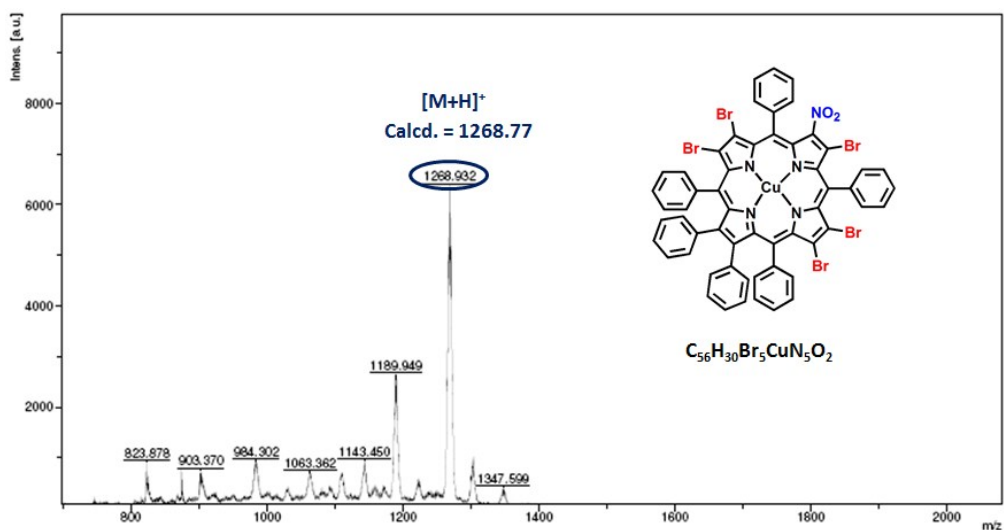


Figure S17. MALDI-TOF mass spectrum of CuTPP(NO_2)(Ph)₂Br₅.

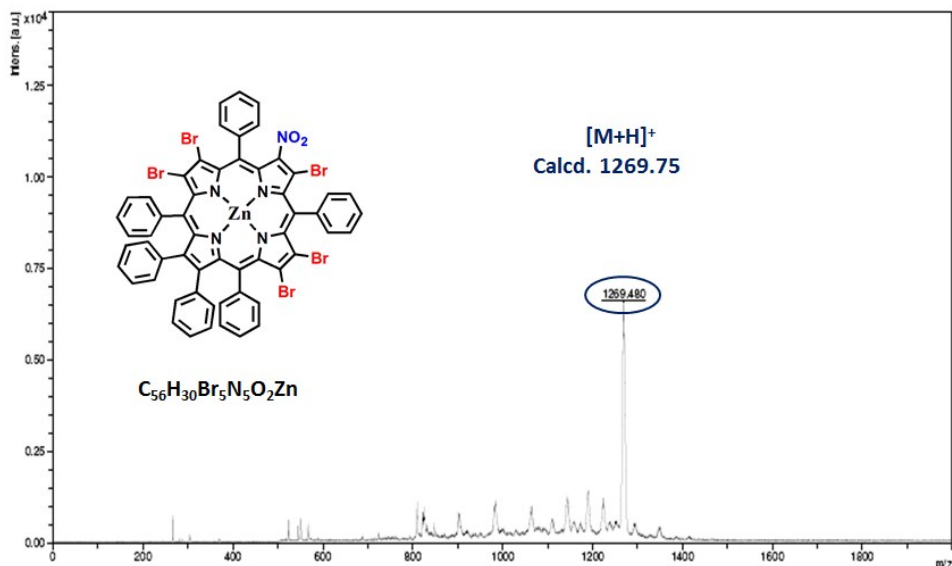


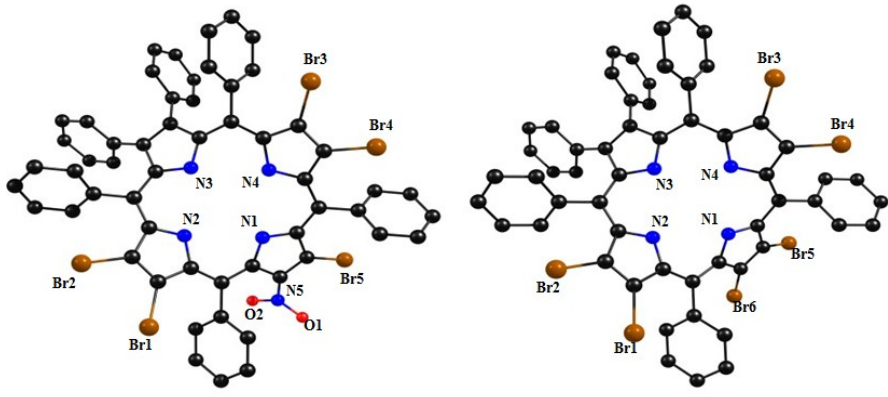
Figure S18. MALDI-TOF mass spectrum of ZnTPP(NO_2)(Ph)₂Br₅.

Table S1. Crystallographic data of H₂TPP(NO₂)(Ph)₂Br₅

	H ₂ TPP(NO ₂)(Ph) ₂ Br ₅
Emperical Formula	C58H40Br5N5O4
Formula wt.	1270.50
Crystal system	Monoclinic
Space group	P 21/c
a (Å)	13.7272(4) Å
b (Å)	27.1133(10) Å
c (Å)	14.7309(5) Å
α (°)	90
β (°)	101.409(2)
γ (°)	90
Volume (Å ³)	5374.4(3) Å ³
Z	4
Dcald (mg/m ³)	1.570 mg/m ³
λ (Å)	0.71073 Å
T (°C)	296(2) K
No. of total reflns.	72230
No. of indepnt. reflns.	9721
R	0.1082
R _w	0.1638
GOOF	1.027
CCDC No.	1921730

Table S2. Selected average bond lengths (\AA) and bond angles ($^{\circ}$) for the single crystal of $\text{H}_2\text{TPP}(\text{NO}_2)(\text{Ph})_2\text{Br}_5$.

Bond Length(\AA)	
	$\text{H}_2\text{TPP}(\text{NO}_2)(\text{Ph})_2\text{Br}_5$
$\text{N}-\text{C}_{\alpha}$	1.354
$\text{N}'-\text{C}_{\alpha'}$	1.311
$\text{C}_{\alpha}-\text{C}_{\beta}$	1.428
$\text{C}_{\alpha'}-\text{C}_{\beta'}$	1.465
$\text{C}_{\beta}-\text{C}_{\beta}$	1.366
$\text{C}_{\beta'}-\text{C}_{\beta'}$	1.273
$\text{C}_{\alpha}-\text{C}_m$	1.411
$\text{C}_{\alpha'}-\text{C}_m$	1.332
$\Delta \text{C}_{\beta} (\text{\AA})$	1.23
$\Delta 24 (\text{\AA})$	0.558
Bond Angle (deg)	
$\text{N}-\text{C}_{\alpha}-\text{C}_m$	125.42
$\text{N}'-\text{C}_{\alpha'}-\text{C}_m$	119.01
$\text{N}-\text{C}_{\alpha}-\text{C}_{\beta}$	106.88
$\text{N}'-\text{C}_{\alpha}-\text{C}_{\beta'}$	111.35
$\text{C}_{\beta}-\text{C}_{\alpha}-\text{C}_m$	127.53
$\text{C}_{\beta'}-\text{C}_{\alpha'}-\text{C}_m$	129.60
$\text{C}_{\alpha}-\text{C}_m-\text{C}_{\alpha'}$	123.34
$\text{C}_{\alpha}-\text{C}_{\beta}-\text{C}_{\beta}$	107.63
$\text{C}_{\alpha'}-\text{C}_{\beta}-\text{C}_{\beta'}$	106.01
$\text{C}_{\alpha}-\text{N}-\text{C}_{\alpha}$	110.94
$\text{C}_{\alpha'}-\text{N}'-\text{C}_{\alpha'}$	105.16

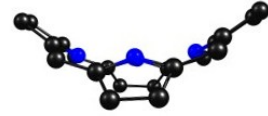


(a)

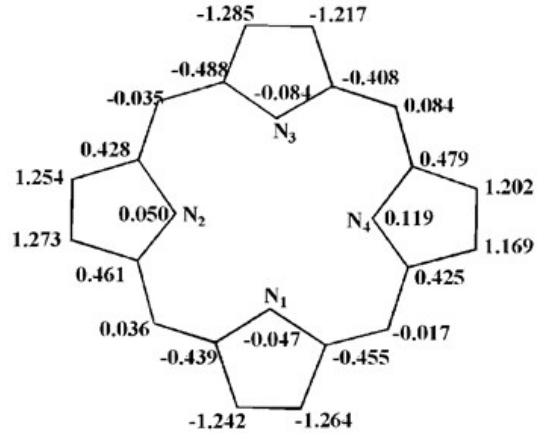
(d)



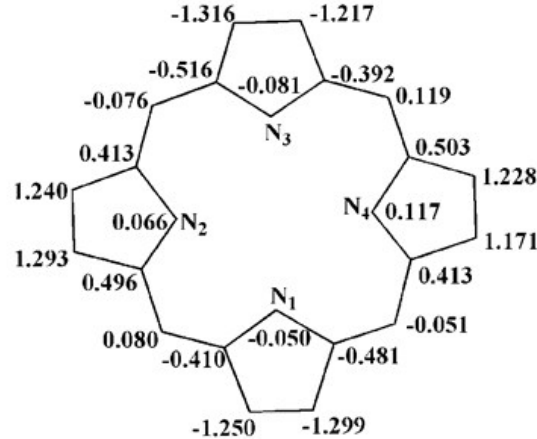
(b)



(e)



(c)



(f)

Figure S19. B3LYP/LANL2DZ- optimized geometry showing the Top views as well as side views of $\text{H}_2\text{TPP}(\text{NO}_2)(\text{Ph})_2\text{Br}_5$ (1a and 1b) and $\text{H}_2\text{TPP}(\text{Ph})_2\text{Br}_6$ (1d and 1e) respectively. The displacement of porphyrin-core atoms from mean plane are shown in figures 1c and 1f for $\text{H}_2\text{TPP}(\text{NO}_2)(\text{Ph})_2\text{Br}_5$ and $\text{H}_2\text{TPP}(\text{Ph})_2\text{Br}_6$ respectively.

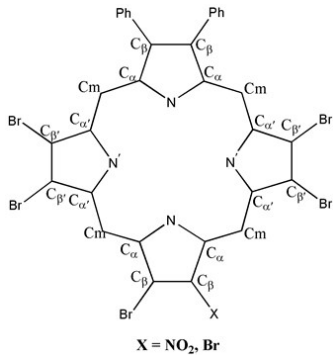


Table S3. Selected bond lengths (\AA) and bond angles ($^\circ$) for the B3LYP/LANL2DZ optimized geometries of $\text{H}_2\text{TPP}(\text{Ph})_2\text{Br}_5\text{X}$ ($\text{X} = \text{NO}_2$ or Br).

	$\text{H}_2\text{TPP}(\text{Ph})_2\text{Br}_6$	$\text{H}_2\text{TPP}(\text{NO}_2)(\text{Ph})_2\text{Br}_5$
Bond Length (\AA)		
$\text{N}-\text{C}_\alpha$	1.385	1.384
$\text{N}'-\text{C}_\alpha'$	1.391	1.391
$\text{C}_\alpha-\text{C}_\beta$	1.477	1.475
$\text{C}_\alpha'-\text{C}_\beta'$	1.450	1.451
$\text{C}_\beta-\text{C}_\beta$	1.382	1.384
$\text{C}_\beta'-\text{C}_\beta'$	1.393	1.391
$\text{C}_\alpha-\text{C}_m$	1.426	1.427
$\text{C}_\alpha'-\text{C}_m$	1.420	1.418
$\Delta\text{C}_\beta (\text{\AA})$	1.251	1.238
$\Delta\text{Z4} (\text{\AA})$	0.594	0.581
Bond Angle (deg)		
$\text{N}-\text{C}_\alpha-\text{C}_m$	122.80	123.13
$\text{N}'-\text{C}_\alpha'-\text{C}_m$	123.45	123.45
$\text{N}-\text{C}_\alpha-\text{C}_\beta$	109.64	109.64
$\text{N}'-\text{C}_\alpha'-\text{C}_\beta'$	105.05	105.09
$\text{C}_\beta-\text{C}_\alpha-\text{C}_m$	127.26	118.81
$\text{C}_\beta'-\text{C}_\alpha'-\text{C}_m$	131.43	131.31
$\text{C}_\alpha-\text{C}_m-\text{C}_\alpha'$	121.90	121.84
$\text{C}_\alpha-\text{C}_\beta-\text{C}_\beta$	106.59	106.58
$\text{C}_\alpha'-\text{C}_\beta'-\text{C}_\beta'$	108.51	108.50
$\text{C}_\alpha-\text{N}-\text{C}_\alpha$	106.89	107.00
$\text{C}_\alpha'-\text{N}'-\text{C}_\alpha'$	112.47	112.41

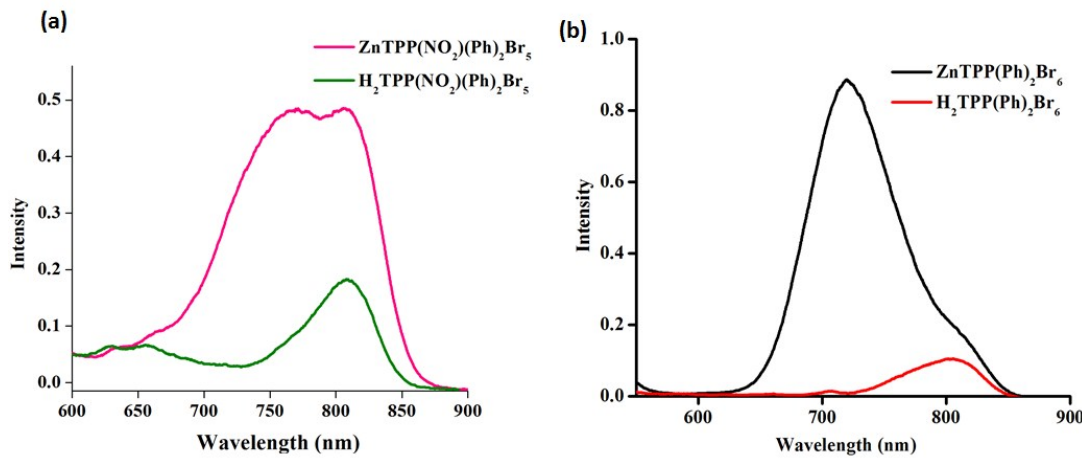


Figure S20. Fluorescence spectra of (a) MTPP(NO_2)(Ph)₂Br₅ and (b) MTPP(Ph)₂Br₆ ($M = 2\text{H}$, Zn (II)) in CH_2Cl_2 at 298 K

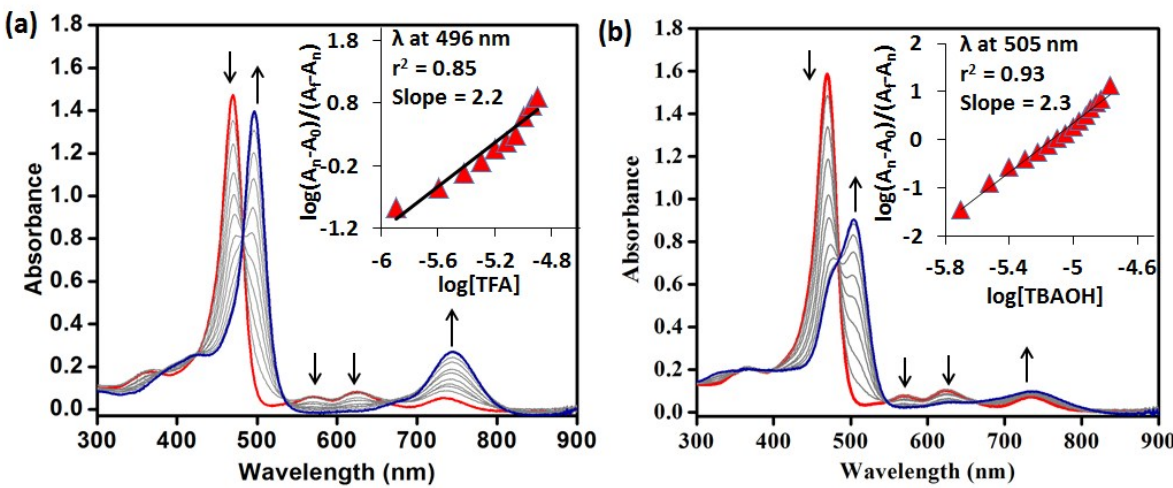


Figure S21. UV-visible spectral titration of H₂TPP(Ph)₂Br₆ with TFA (a) and TBAOH (b) in toluene at 298 K respectively. Insets shows the corresponding Hill plots.

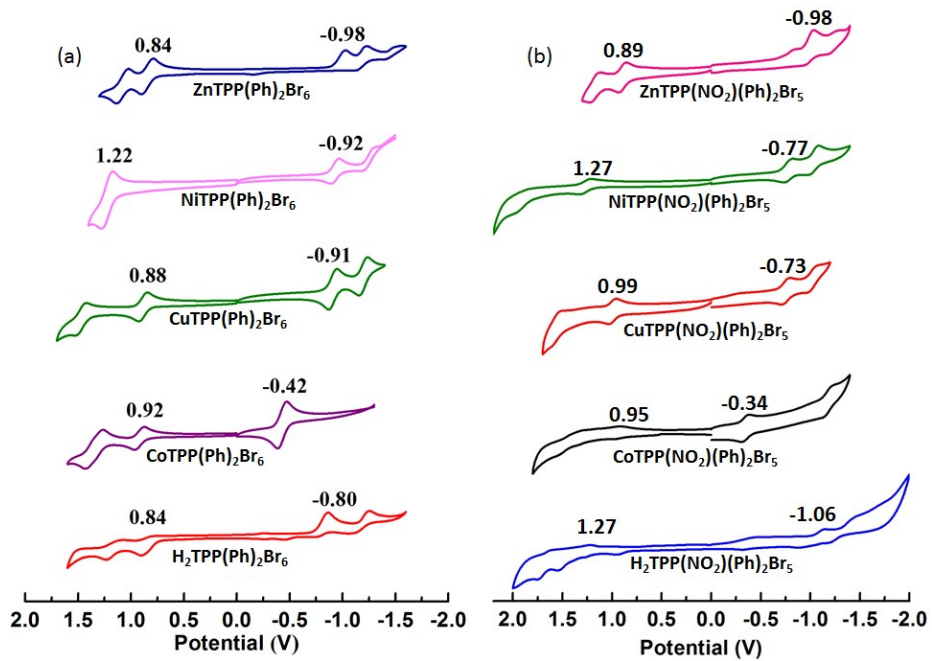


Figure S22. Cyclic Voltametric (in V vs Ag/ AgCl) traces recorded for porphyrins (a) MTPP(Ph)₂Br₆(M = 2H, Co(II), Cu(II), Ni(II), Zn(II)) and (b) MTPP(NO₂)(Ph)₂Br₅(M = 2H, Co(II), Cu(II), Ni(II), Zn(II)) in CH₂Cl₂ containing 0.1 M TBAPF₆ with a scan rate of 0.1 V/s at 298 K.